

Efficient Diagonalization of Kicked Quantum Systems

R. Ketzmerick,^{1,2} K. Kruse,² and T. Geisel^{1,2}

¹*Institute for Theoretical Physics, University of California, Santa Barbara, CA 93106, USA*

²*Max-Planck-Institut für Strömungsforschung und Institut für Nichtlineare Dynamik der Universität Göttingen, Bunsenstraße 10, D-37073 Göttingen, Germany**

We show that the time evolution operator of kicked quantum systems, although a full matrix of size $N \times N$, can be diagonalized with the help of a new method based on a suitable combination of Fast Fourier Transform and Lanczos algorithm in just $O(N^2 \ln N)$ operations. It allows the diagonalization of matrices of sizes up to $N \approx 10^6$ going far beyond the possibilities of standard diagonalization techniques which need $O(N^3)$ operations. We have applied this method to the kicked Harper model revealing its intricate spectral properties.

PACS numbers: 02.60.Dc, 05.45.+b

I. INTRODUCTION

Periodically kicked quantum systems have played a prominent role in studies of quantum chaos [1] for the analysis of signatures of classical chaos in quantum systems [2]. Important examples are the kicked rotator, i.e., the quantum version of Chirikov's standard map [1,3], the kicked top [2], and the kicked Harper model [4]. Their quantum time evolution operator allows a fast numerical iteration on wave packets just like in their classical analogs, which are maps that can be iterated very quickly. The study of kicked systems has led to many discoveries, a very spectacular one being the suppression of classical chaotic diffusion due to quantum mechanical interference in the kicked rotator [1], which later on was understood by a mapping onto the Anderson model of disordered systems [5] and onto the supersymmetric nonlinear σ model for quasi one-dimensional wires [6]. Another example supporting the importance of kicked systems appeared in the study of quantum signatures of classical

chaos in quasiperiodic systems, in which the kicked Harper model [4,7–18] yielded surprising phenomena [8,11,12,17,18], e.g., metal-insulator transitions tuned by classical chaos. In the future, kicked quantum systems most probably will be the first to be used for numerical studies of the quantum signatures of mixed systems having a hierarchical phase space structure at the boundary between regular and chaotic motion. For example, the semiclassicalally predicted [19] and experimentally observed [20,21] fractal properties of conductance fluctuations wait to be verified by numerical quantum calculations.

In this paper we will show how the Lanczos algorithm for diagonalizing matrices [22], which is well suited for *sparse* matrices, can be used to exploit the advantages of kicked quantum systems even though their time evolution operator is a *full* matrix. The key point, which has been overlooked throughout twenty years of studying quantum chaos with kicked systems, is the following observation: The most time consuming step of the Lanczos algorithm, a matrix-vector multiplication, is analogous to a step of the time evolution for some wave packet. For kicked systems the time evolution is known to be efficiently performed by using the Fast Fourier Transform (FFT) algorithm [23]. Consequently, by combining the Lanczos algorithm and the FFT, diagonalization of kicked systems only takes of the order of $N^2 \ln N$ operations and for a matrix of size $N = 10^5$ needs about two days on a standard workstation. By using parallel computers matrices of size $N = 10^6$ should be diagonalizable.

As a first application of this new method, we will study the quantum signatures of classical chaos in quasiperiodic systems. For the kicked Harper model (KHM) *off* the critical line, Borgonovi and Shepelyansky [17] convincingly concluded from diagonalizing matrices of sizes up to $N = 1775$ that in the limit $N \rightarrow \infty$ the spectrum, in addition to pure point and absolutely continuous components, can also have a singular continuous component. The Lanczos-FFT method allows us to easily diagonalize the KHM for the much larger size of $N = 51536$. We will show that the indications for a singular continuous component found in Ref. [17] do not persist for larger system sizes. We will thereby reveal the KHM's intricate spectral properties and demonstrate the applicability of our method.

II. THE LANCZOS-FFT METHOD

The numerical advantage of the time evolution of a periodically kicked system, e.g., a one-dimensional Hamiltonian of the form

$$H(t) = T(p) + V(x) \sum_n \delta(t - n), \quad (1)$$

is due to the fact, that its time-evolution operator for one period factorizes into

$$U = \exp \left\{ -\frac{i}{\hbar} T(p) \right\} \exp \left\{ -\frac{i}{\hbar} V(x) \right\}. \quad (2)$$

Here, \hbar is typically an *effective* Planck's constant, p is the momentum and x the position operator. The second factor describes the kick, whereas the first factor governs the free evolution between kicks. If U is periodic in x , then U can be represented as an infinite matrix depending on a Bloch phase θ_x , the so-called quasi-momentum. If, in addition, U is periodic with period N , i.e., $U_{l+N, l'+N} = U_{l, l'}$, the time-evolution operator can be reduced to an $N \times N$ matrix depending on a second Bloch phase θ_p . This is, e.g., the case for the kicked rotator and the kicked Harper model, when \hbar takes the value $2\pi M/N$. In order to obtain the time evolution it will be applied iteratively to a wave packet described by a vector of length N . This application in general requires N^2 operations for a single time step, whereas the factorization of U [Eq. (2)] allows a much faster implementation: In either momentum or position representation, application of the first and second factor of U , resp., amounts to a vector-vector multiplication using just N operations. Going back and forth between position and momentum representation one uses the very efficient FFT algorithm, which needs of the order of $N \ln N$ operations [23]. A detailed description of this standard method is given in the appendix including its extension to cases where N is not a power of 2. Thus, for propagating a wave packet one period in time just $O(N \ln N)$ operations are needed, which allows the study of time evolutions in systems with sizes up to $N \approx 10^6$.

On the other hand, this dramatic advantage of kicked quantum systems when studying time evolutions has not yet been fully exploited for determining the *eigenvalues* of U . So far this advantage has been used in this context to perform the time evolution for zN steps

taking just $zN^2 \ln N$ operations and to Fourier transform the resulting time series giving the unitary eigenvalues. Unfortunately, for large matrices this method fails for two reasons: (i) resolution: very often, the finite resolution $1/(zN)$ will not resolve closeby eigenvalues. Even worse, for quasiperiodic quantum systems with fractal spectra of dimension $D < 1$, in which the typical level spacing scales as $1/N^{1/D}$, this requires at least $O(N^{1+1/D} \ln N)$ operations. (ii) storage: if U has localized eigenfunctions, one needs to store the time evolution at $O(N)$ sites and needs storage of $O(zN^2)$ bytes, which for $N = 10^6$ and a relatively small $z = 10$ amounts to 10^5 Gigabyte by far exceeding conventional storage capacities. Standard diagonalization methods need $O(N^3)$ operations and have so far restricted N to values of only a few thousand.

We will now describe explicitly the algorithm which makes use of the factorization of U [Eq. (2)] to obtain all eigenvalues in $O(N^2 \ln N)$ operations. To this end we start by recalling the standard Lanczos algorithm for a general $N \times N$ complex Hermitian matrix H [22]. It generates a sequence of *tridiagonal* real symmetric matrices

$$L_n = \begin{pmatrix} \alpha_1 & \beta_2 & & & \\ \beta_2 & \alpha_2 & \ddots & & \\ & \ddots & \ddots & \beta_n & \\ & & \beta_n & \alpha_n & \end{pmatrix}, \quad (3)$$

whose eigenvalues can be calculated very efficiently by standard routines [23] and converge towards the eigenvalues of H . The calculation of α_n and β_n is based on the following recursion relations: Let $\psi_0, \psi_1 \in \mathbb{C}^N$ with $\psi_0 \equiv 0$ and ψ_1 a normalized random vector. Then for $n \geq 1$ we have $\alpha_n = (\psi_n, H\psi_n)$, $\beta_n = (\psi_n, H\psi_{n-1})$, and $\psi_{n+1} = \bar{\psi}_{n+1}/\|\bar{\psi}_{n+1}\|$, where $\bar{\psi}_{n+1} = H\psi_n - \alpha_n\psi_n - \beta_n\psi_{n-1}$. If the calculation is carried out in exact arithmetic, then L_N has the same eigenvalues as H . In fact, in this case L_N is related to H via a similarity transformation Ψ , i.e., $\Psi^{-1}H\Psi = L_N$ with $\Psi = (\psi_1 \dots \psi_N)$. Due to the instability of the algorithm for finite precision arithmetic, n has to be larger than N in order to approximate all eigenvalues of H with sufficient accuracy. In this case, L_n will possess spurious eigenvalues not approximating any eigenvalue of H . These so-called ghosts can be

detected efficiently using standard techniques [22]. Even though this algorithm is designed for Hermitian matrices it can be used to obtain the spectrum of a unitary matrix U by applying it to $H^+ = \frac{1}{2}(U + U^\dagger)$ and $H^- = \frac{1}{2i}(U - U^\dagger)$. Then, for an eigenvalue $e^{i\omega}$ of U the eigenvalues of H^+ and H^- are $\cos \omega$ and $\sin \omega$, resp.

The most time consuming step in each iteration of the Lanczos algorithm is the calculation of $H\psi_n$ which in general needs N^2 operations. If $H\psi_n$ can be computed in fewer operations as is the case for sparse matrices, the algorithm will become faster than standard diagonalization techniques. As described above, for kicked systems in which U is a *full* matrix, one can make use of its factorization [Eq.(2)] and the FFT algorithm to calculate $U\psi_n$ and thus $H^\pm\psi_n$ in just $O(N \ln N)$ operations. Hence, by using the Lanczos-FFT method the eigenvalues of U can be calculated in $O(N^2 \ln N)$ operations, such that systems of sizes up to $N \approx 10^6$ are treatable.

Let us finally mention that the numerical workload may be further reduced if U obeys certain symmetries. i) If the $N \times N$ matrix U is symmetric, then $H^+ = \text{Re}U$ and $H^- = \text{Im}U$ such that U^\dagger no longer occurs. This is, e.g., the case for the kicked Harper model if one uses the time evolution operator U for one period starting halfway between two kicks with $\theta_p = 0$. The spectrum, of course, is independent of the chosen time when the one period time evolution operator starts. ii) If the eigenvalues $e^{i\omega}$ of U are symmetric with respect to $\omega = 0$, it suffices to diagonalize H^+ . Each of these symmetries reduces the number of operations by a factor of 2. This completes the description of our method to determine the spectrum of a kicked quantum system in $O(N^2 \ln N)$ operations.

III. THE SPECTRUM OF THE KICKED HARPER MODEL

We will now apply the Lanczos-FFT method to the kicked Harper model (KHM) [4,7–18]. By calculating the quasienergies of a system of size $N \approx 50000$ we will give strong evidence that a former result on the spectral properties of the KHM obtained by treating matrices of sizes up to $N \approx 2000$ cannot be maintained. Since kicked systems with a larger size can

up to now only be treated by the Lanczos-FFT method, this demonstrates the value of this algorithm.

As a generalization of the Harper model [25–27] the KHM is widely used to study the influence of a chaotic classical limit on the spectral properties of a quasiperiodic quantum system [8,11,12,17,18]. The Harper model is described by a tight-binding Hamiltonian with potential $V_n = V \cos(2\pi\sigma n + \nu)$ at site n . The Hamiltonian of the KHM is given by

$$H = L \cos p + K \cos x \sum_n \delta(t - n), \quad (4)$$

i.e., it is of the form (1) with $T(p) = L \cos p$ and $V(x) = K \cos x$. For small values of K and L its spectrum is closely related to the spectrum of the Harper model [9]. To be explicit, for small L/\hbar and K/\hbar the quasienergies of the KHM are given up to a factor $L/2\hbar$ by the eigenenergies of the Harper model with $V = 2K/L$, $\sigma = \hbar/2\pi$ and $\nu = \theta_x$. Therefore, in the case of small K and L the spectral properties of the KHM are the same as for the Harper model: For a typical irrational $\hbar/2\pi$ and fixed quasimomentum θ_x the spectrum is pure point if $K > L$, absolutely continuous if $L > K$, and singular continuous for $K = L$ with a fractal dimension given by that of the Harper model. Due to a duality property of the KHM [28] on the critical line $K = L$, the spectrum remains singular continuous for all values of $K = L$. Its fractal dimension, though, changes with increasing K [11]. Off the critical line, for increasing values of K and L the spectral properties of the KHM differ from the Harper model in that in some regions pure point and absolutely continuous components coexist [8,12]. The changes in the spectral type for $K \neq L$ can be understood with the help of avoided band crossings (ABCs) [18]. These are present in the spectrum of the KHM because its classical version generates chaotic dynamics (see Fig. 5 in Ref. [18]). As has been shown in Ref. [18] they may tune metal-insulator transitions, thus explaining the coexistence of pure point and absolutely continuous spectral components. Since the fractal dimensions of a spectrum may also change due to ABCs [18], they provide a common explanation for all the changes in the quasienergy spectrum of the KHM mentioned above.

Based on a numerical analysis of matrices of sizes up to $N = 1775$, Borgonovi and

Shepelyansky found indications that even a singular continuous component should exist off the critical line [17]. In particular, they have studied the case of $K = 4$, $L = 7$, $\hbar = 2\pi/(6 + \sigma_G)$, where $\sigma_G = (\sqrt{5} + 1)/2$ is the Golden Mean. For these parameters they have calculated the inverse participation ratio $\xi = \sum_n |\psi_n|^4$ of the eigenfunctions ψ for the approximants $2\pi 55/419$, $2\pi 144/1097$ and $2\pi 233/1775$ of $\hbar = 2\pi/(6 + \sigma_G)$ yielding matrices of sizes $N = 419, 1097$ and 1775 , resp. In some regions of the spectrum they have found the inverse participation ratio of the corresponding eigenfunctions to decrease as N^{-1} , indicating that there the spectrum is absolutely continuous, while in other regions the inverse participation ratio remains constant, indicating the spectrum to be pure point. Most interestingly, for quasienergies in the interval $[2.4, 2.8]$ the inverse participation ratio of the corresponding eigenfunctions scaled with some exponent larger than -1 and smaller than 0, indicating a singular continuous spectral component in the limit $N \rightarrow \infty$.

Using the Lanczos-FFT method we have calculated the quasienergy spectrum for the same values of K and L but for $\hbar = 2\pi 6765/51536$ that is a much higher approximant of $2\pi/(6 + \sigma_G)$. This yields a matrix of size $N = 51536$, by far exceeding the size of a matrix treatable by standard methods. In Fig. 1 we show the quasienergy spectrum versus the Bloch-phase θ_x and several magnifications of the quasienergy interval $[2.4, 2.8]$. Note that the isolated dots present in the figure are ghosts produced by the Lanczos algorithm. From a plot of the eigenvalues of a periodic approximant as given here, one can infer the spectral type of the quasiperiodic system as follows: The spectrum is pure point if the width of Bloch bands is negligible as compared to their spacings. It is absolutely continuous if the spacings are negligible compared to the band widths. The self-similar structure of a singular continuous spectrum leads to band widths and spacings of comparable size as can be found, e.g., for the Harper model at the critical point. In Fig. 1 on intermediate scales the spectrum displays a self-similar structure in the quasienergy interval $[2.4, 2.8]$, confirming the findings of Ref. [17]. As the final magnifications show, however, on smaller scales the self-similarity vanishes in many places and there the spectrum consists of either levels or bands corresponding to pure point and absolutely continuous components, resp. Note, however,

that we also find small regions, where the self-similarity does not end even for our large matrix size (not shown in Fig. 1). This indicates that the fraction of self-similar scaling regions is decreasing with matrix size and questions the occurrence of a singular continuous component in the limit $N \rightarrow \infty$. How can one understand this surprising property of the KHM?

This self-similar structure of the spectrum on intermediate scales can be understood with the help of avoided band crossings. As already mentioned, ABCs tune metal-insulator transitions in the KHM leading to the coexistence of pure point and absolutely continuous components of the spectrum for $K \neq L$. Numerical investigations show that these components do not overlap. Hence, there will be a transition manifold in the $(\text{quasienergy}, K, L)$ -space separating pure point from absolutely continuous regions. If this transition manifold, which may have a very complicated shape, would coincide with a line of fixed K and L over some quasienergy region, one would have a singular continuous component in this spectral region. Unless there is a special symmetry present (like for $K = L$), however, this is very unlikely to happen. Typically, a line of fixed K and L will have many *intersections* with this manifold, yielding quasienergy regions with either pure point or absolutely continuous spectrum. Thus there is no singular continuous component but the absolutely continuous and pure point components can be intermingled in a complicated manner depending on the shape of the transition manifold. The closer one is to an intersection with the transition manifold, the finer will be the scale where the self-similar looking spectrum decides for being pure point or absolutely continuous. For this reason the spectrum looks self-similar on intermediate scales, whereas on smaller scales pure point and absolutely continuous components show up. This is just what can be seen in the quasienergy spectrum shown in Fig. 1. This also explains why for some regions of the spectrum that are even closer to such an intersection, we find self-similar structure on all scales of our finite matrix. In the limit of an infinite matrix size the fraction of self-similar scaling regions should tend to zero and there should be no singular continuous component.

In order to go beyond this qualitative understanding, we plan for the future to study

quantitatively how this fraction decays. Also, it will be interesting to map out the transition manifold in the (quasienergy, K, L)-space by studying the spectrum for large matrices. One may wonder if it has a finite or an infinite number of intersections with a line of fixed K and L .

IV. CONCLUDING REMARKS

In this article we have presented a very powerful method for diagonalizing kicked quantum systems of sizes up to $N \approx 10^5$ on standard present day workstations. The necessity of diagonalizing matrices of this size was then demonstrated by the example of the KHM. Its intricate spectral structure was revealed and found to have its reason in the occurrence of avoided band crossings. As was alluded to in the introduction, the possibility of obtaining the eigenvalues of large matrices is of great interest also in other areas of quantum chaos. Currently, our method is applied to the investigation of quantum fractal eigenstates [24]. In the future, some possible applications include the study of level statistics for very large spacings, the search for quantum signatures of the hierarchical phase space of mixed systems, and the study of predictions for disordered systems via the kicked rotator [6]. We express our hope that the Lanczos-FFT method will play a useful role in the field of quantum chaos.

This research was carried out partially during two of the authors' stay at the Institute for Theoretical Physics, Santa Barbara. T. G. and R. K. gratefully acknowledge the hospitality of the ITP and its members. It was supported by the NSF under Grant No. PHY94-07194 and in part by the Deutsche Forschungsgemeinschaft.

V. APPENDIX

In this appendix we give the explicit expressions usually employed for calculating $U\psi$, when U may be factorized according to Eq. (2). In, e.g., momentum representation we have

$$U = \exp \left\{ -\frac{i}{\hbar} T(p) \right\} F_{p \leftarrow x} \exp \left\{ -\frac{i}{\hbar} V(x) \right\} F_{x \leftarrow p}, \quad (5)$$

with the effective Planck's constant \hbar and $F_{p \leftarrow x}$ and $F_{x \leftarrow p}$ denoting the Fourier transform from position to momentum space and vice versa, resp. If the first and the third factor on the r.h.s. are periodic with period N , the operator reduces to a matrix of size $N \times N$ depending on two Bloch phases. Then, these factors are diagonal matrices with elements $\exp \left\{ -\frac{i}{\hbar} T \left(\hbar \left(l + \frac{\theta_x}{2\pi} \right) \right) \right\}$ and $\exp \left\{ -\frac{i}{\hbar} V \left(2\pi \left(k + \frac{\theta_p}{2\pi} \right) / N \right) \right\}$, resp., in which $k, l = 0, \dots, N-1$, and $\theta_x, \theta_p \in [0, 2\pi]$ are the Bloch phases in position and momentum representation, resp. The Fourier transform $F_{p \leftarrow x}$ is the matrix

$$(F_{p \leftarrow x})_{lk} = \frac{1}{\sqrt{N}} e^{-2\pi i \left(l + \frac{\theta_x}{2\pi} \right) \left(k + \frac{\theta_p}{2\pi} \right) / N} \quad (6)$$

$$= e^{-i\theta_x \theta_p / 2\pi N} e^{-ik\theta_x / N} \frac{1}{\sqrt{N}} e^{-2\pi i k l / N} e^{-il\theta_p / N} \quad (7)$$

which factorizes in a scalar, in two diagonal matrices, and a standard Fourier transform, which can be implemented using the FFT algorithm. $(F_{x \leftarrow p})_{kl}$ is simply the conjugate complex of $(F_{p \leftarrow x})_{lk}$ such that in the final expression for U [Eq.(5)] the first two terms of Eq.(7) cancel each other.

The advantage of using the FFT algorithm exists only if N is a power of 2; otherwise it is less efficient. In situations where N is not a power of 2, as is typically the case for the kicked Harper model where an irrational value of $\hbar/2\pi$ is approximated by a rational M/N , one may use the following strategy: One replaces the Fourier transforms in \mathbb{C}^N by Fourier transforms in $\mathbb{C}^{\tilde{N}}$ where $\tilde{N} > 2N$ is a power of 2. Before the first FFT one extends the vector of size N to a vector of size \tilde{N} by adding zeros and after the second FFT one retains only the first N elements of the resulting vector. In addition, one has to replace the diagonal matrix of size $N \times N$ with elements $\exp \left\{ -\frac{i}{\hbar} V \left(2\pi \left(k + \frac{\theta_p}{2\pi} \right) / N \right) \right\}$ by a diagonal matrix of size $\tilde{N} \times \tilde{N}$ with elements

$$\frac{1}{N} \sum_{j=-N+1}^{N-1} \sum_{m=0}^{N-1} \exp \left\{ -\frac{i}{\hbar} V \left(2\pi \left(m + \frac{\theta_p}{2\pi} \right) / N \right) \right\} e^{-2\pi i j l / N} e^{2\pi i j k / \tilde{N}}, \quad (8)$$

in which $k = 0, \dots, \tilde{N} - 1$.

REFERENCES

* Present and permanent address.

- [1] G. Casati, B. V. Chirikov, F. M. Izraelev, and J. Ford, in *Stochastic Behavior in Classical and Quantum Hamiltonian Systems* Vol. 93 of *Lecture Notes in Physics*, edited by C. Casati and J. Ford (Springer, New York, 1979).
- [2] See e.g., F. Haake, *Quantum Signatures of Chaos*, Springer Series in Synergetics, Vol. 54 (Springer-Verlag, Berlin Heidelberg, 1991); G. Casati and B. Chirikov (eds.), *Quantum Chaos: Between order and disorder* (Cambridge University Press, 1995).
- [3] F. Izrailev, Phys. Rep. **196** (1990) 299.
- [4] R. Artuso, G. Casati, F. Borgonovi, L. Rebuzzini, and I. Guarneri, Int. J. Mod. Phys. B **8** (1994) 207.
- [5] S. Fishman, D. R. Grempel, and R. E. Prange, Phys. Rev. Lett. **49** (1982) 509.
- [6] A. Altland and M. R. Zirnbauer, Phys. Rev. Lett. **77** (1996) 4536.
- [7] P. Leboeuf, J. Kurchan, M. Feingold, and D. P. Arovas, Phys. Rev. Lett. **65** (1990) 3076.
- [8] R. Lima and D. Shepelyansky, Phys. Rev. Lett. **67** (1991) 1377.
- [9] T. Geisel, R. Ketzmerick, and G. Petschel, Phys. Rev. Lett. **67** (1991) 3635.
- [10] R. Ketzmerick, G. Petschel, and T. Geisel, Phys. Rev. Lett. **69** (1992) 695.
- [11] R. Artuso, G. Casati, and D. Shepelyansky, Phys. Rev. Lett. **68** (1992) 3826.
- [12] R. Artuso, F. Borgonovi, I. Guarneri, L. Rebuzzini, and G. Casati, Phys. Rev. Lett. **69** (1992) 3302.
- [13] I. Guarneri and F. Borgonovi, J. Phys. **A26** (1993) 119.
- [14] R. Roncaglia, L. Bonci, F. M. Izrailev, B. J. West, and P. Grigolini, Phys. Rev. Lett. **73** (1994) 802.

- [15] P. Leboeuf and A. Mouchet, Phys. Rev. Lett. **73** (1994) 1360.
- [16] I. Dana, Phys. Rev. Lett. **73** (1994) 1609.
- [17] F. Borgonovi and D. Shepelyansky, Europhys. Lett **29** (1995) 117.
- [18] R. Ketzmerick, K. Kruse, and T. Geisel, Phys. Rev. Lett., **80** (1998) 137.
- [19] R. Ketzmerick, Phys. Rev. B **54** (1996) 10841.
- [20] H. Hegger et al., Phys. Rev. Lett. **77**, (1996) 3885.
- [21] A. S. Sachrajda et al., Phys. Rev. Lett. **80** (1998) 1948.
- [22] J. K. Cullum and R. A. Willoughby, *Lanczos Algorithms for Large Symmetric Eigenvalue Computations*, Progress in Scientific Computing, Vol. 3 (Birkhäuser, Boston, 1985).
- [23] W. H. Press, S. A. Teukolsky, W. T. Vetterling, and B. P. Flannery, *Numerical Recipes*, 2nd ed. (Cambridge University Press, 1992).
- [24] G. Casati, G. Maspero, and D. Shepelyansky, www site <http://xxx.lanl.gov/abs/cond-mat/9710118>.
- [25] P. G. Harper, Proc. Roy. Soc. London **A68** (1955) 874.
- [26] M. Y. Azbel, Sov. Phys. JETP **19** (1964) 634.
- [27] D. R. Hofstadter, Phys. Rev. B **14** (1976) 2239.
- [28] J. Bellissard and A. Barelli, in *Quantum Chaos - Quantum Measurement*, edited by P. Cvitanović, I. C. Percival, and A. Wirzba (Kluwer Academic Publishers, Dordrecht 1992).

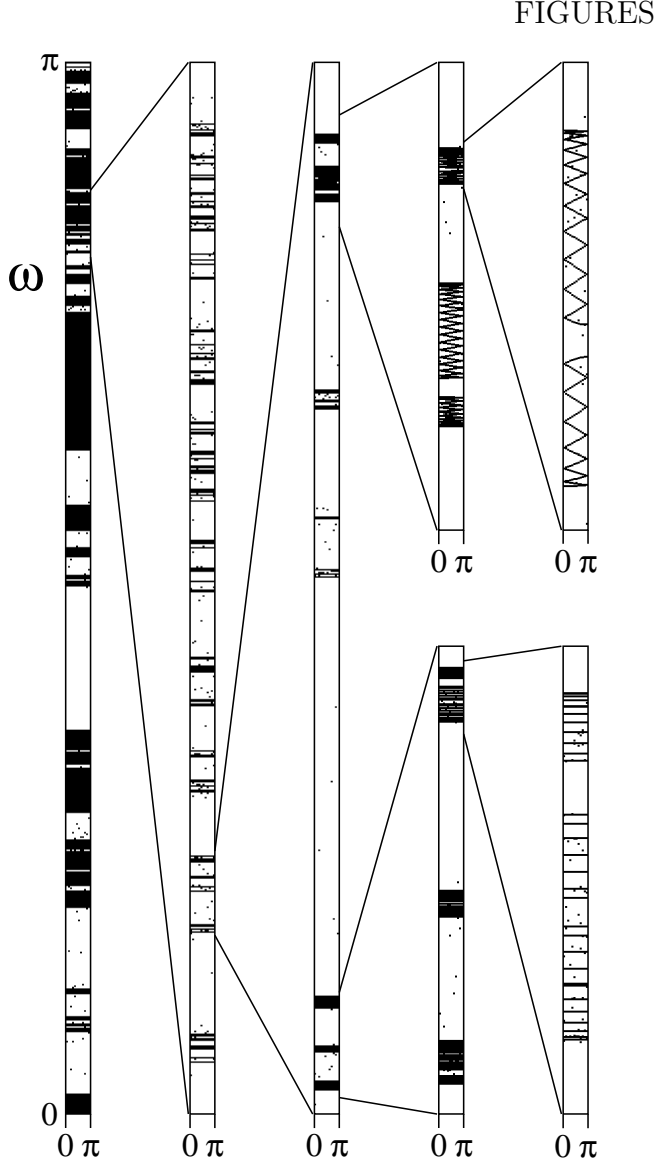


FIG. 1. Quasienergies ω vs. Bloch phase $\theta_x N$ of the kicked Harper model [Eq.(4)] for $K = 4$, $L = 7$, $\hbar = 2\pi \cdot 6765/51536$, and $\theta_p = 0$. Successive magnifications show fractal behaviour on several scales, whereas the last magnification reveals either localized eigenfunctions (no phase dependence of the quasienergies) or extended eigenfunctions (strong phase dependence and no visible gaps). The magnifications are for the intervals [2.56, 2.76], [2.594, 2.61], [2.6076, 2.6092], [2.60874, 2.60891], [2.59425, 2.59585] and [2.59555, 2.5958]. The isolated points are ghosts due to the instability of the Lanczos algorithm.